

---

---

REMOTE SENSING OF ATMOSPHERE,  
HYDROSPHERE, AND UNDERLYING SURFACE

---

---

## Mesoscale ( $\beta$ and $\gamma$ ) Inhomogeneities of Atmospheric Composition over Tomsk

M. Yu. Arshinov<sup>a</sup>, B. D. Belan<sup>a,\*</sup>, S. B. Belan<sup>a</sup>, D. K. Davydov<sup>a</sup>, A. V. Kozlov<sup>a</sup>, and O. O. Marchenko<sup>a</sup>

<sup>a</sup> V.E. Zuev Institute of Atmospheric Optics, Siberian Branch, Russian Academy of Sciences, Tomsk, 634055 Russia

\*e-mail: bbd@iao.ru

Received March 23, 2025; revised April 1, 2025; accepted April 9, 2025

**Abstract**—According to the conclusions of the UN Intergovernmental Panel on Climate Change, to determine the main causes of the global warming caused by an increase in the content of greenhouse gases in the atmosphere, an accurate assessment of their emissions and sinks is required. However, there are still significant uncertainties in the estimation of their budget. The present work studies the mesoscale inhomogeneities in the distribution of their fluxes and sinks based on hourly measurements at three air monitoring posts near Tomsk: TOR station, Fonovaya Observatory, and Basic Experimental Complex (BEC). This approach seems promising considering the significant role of soil in gas exchange processes. The differences in long-term (2013–2017) average concentrations between stations are shown to be within the ranges 116–195  $\mu\text{g}/\text{m}^3$  for CO, 3.3–8.3 ppm for CO<sub>2</sub>, 0.4–0.8  $\mu\text{g}/\text{m}^3$  for NO, 4.6–15.5  $\mu\text{g}/\text{m}^3$  for NO<sub>2</sub>, 8.1–14.3  $\mu\text{g}/\text{m}^3$  for O<sub>3</sub>, and 2.3–6.9  $\mu\text{g}/\text{m}^3$  for SO<sub>2</sub>. Annual and daily variations in the concentration differences have been revealed for the first time. The results expand our knowledge about the dynamics of greenhouse and oxidizing gases in the atmosphere and can be useful in developing requirements for their measurement accuracy.

**Keywords:** atmosphere, sulfur dioxide, methane, ozone, nitrogen oxides, carbon oxides, transport, composition

**DOI:** 10.1134/S1024856025700617

### INTRODUCTION

According to the UN Intergovernmental Panel on Climate Change (IPCC), an increase in the atmospheric concentrations of greenhouse and other gases coming from both anthropogenic and natural sources is among the main causes of the global warming [1]. Therefore, accurate estimation of their emissions and sinks and their redistribution between the atmosphere, ocean, and terrestrial biosphere is of crucial importance for developing climate policy and predicting future climate changes. Despite many studies of the budget of greenhouse gases on the planet, there are still significant uncertainties in its assessment [2–4], which is rather because not all sources and sinks are considered in the related calculations. In search of causes of this circumstance, a number of scientists draw attention to mesoscale [5, 6] and even microscale [7, 8] inhomogeneities of the distribution of the fluxes and sinks of greenhouse gases. Considering a significant role of soil in gas exchange processes and its significantly different properties on both scales [9], this seems a promising approach.

The distribution of gas composition of the atmosphere can be also affected by vegetation. On the one hand, it determines surface albedo and heat inflow [10]. On the other hand, grass and trees can be sources

or sinks of gases [11] or their precursors, for example, of ozone [12]. In addition to the heterogeneity of soil and vegetation properties, the distribution of gas composition can be affected by the surface roughness and wind parameters [13, 14].

Another possible cause of the mesoscale heterogeneity of the atmospheric composition distribution is circulation [15], which is induced by two underlying surface heterogeneity types: orographic (relief) and thermal. The orographic heterogeneity causes slope and mountain-valley winds, foehns (including the famous bora), Karman vortex path, and leeward rotors. The thermal heterogeneity is produced by differences in radiative (albedo), thermophysical (thermal conductivity and heat capacity), and aerodynamic (roughness) properties between contrasting underlying surface types. These differences cause different rates of heating and cooling of these surfaces during the day and, hence, different daily amplitudes of the surface temperature. A classic example of mesoscale circulation developing over a thermally heterogeneous underlying surface is breeze circulation (breeze). Thus, there are all prerequisites for mesoscale inhomogeneity of atmospheric composition distribution in the nature.

The study of this mesoscale inhomogeneity is complicated by the fact that gas concentration monitoring

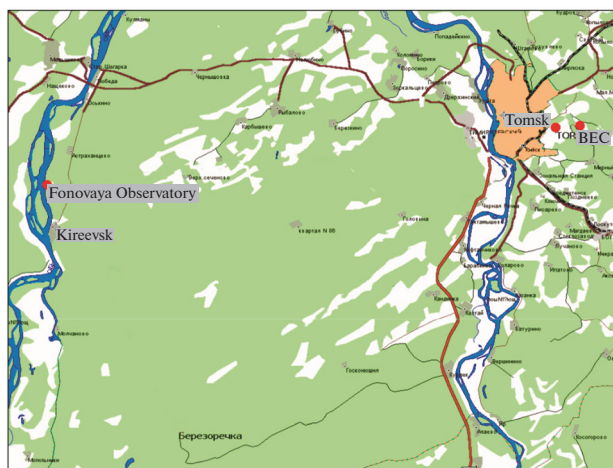


**Fig. 1.** Monitoring posts in the region of Tomsk.

stations are extremely unevenly distributed over land and located far apart from each other. For example, according to [16], variability of greenhouse gas concentrations in the surface air layer is analyzed in the Russian Federation only at four observation stations, which are part of the Global Atmosphere Watch (GAW) program of the WMO. Teriberka (Kola Peninsula, Barents Sea coast) and Tiksi (Arctic coast, Laptev Sea, Sogo Bay) stations are located in background conditions; Novy Port (Yamal Peninsula, Ob Bay coast) and Voeikovo stations (suburb of St. Petersburg) are in regions of large-scale anthropogenic sources of greenhouse gases. That is, there are only two state background stations on the large Russian territory.

The solution to the air monitoring problem was previously connected with the development of satellite sounding systems. Thus, 15 satellite types for measuring the aerosol and gas composition of the atmosphere were already in operation in 2007 [17]. However, the accuracy of satellite data is still insufficient [18, 19]. Numerical simulation of the distribution of greenhouse gas concentrations and fluxes suggests that their heterogeneity can be significant [20, 21], comparable with large-scale variations [22].

We have created several stationary and mobile complexes for measuring greenhouse gas concentrations in Western Siberia with the accuracy meeting WMO requirements. Their positions enable not only large-scale but also mesoscale studies of greenhouse gas distribution. The study of mesoscale heterogeneities of gas composition distribution is the aim of this work. The following questions are considered: what is the scale where significant differences in greenhouse gas concentrations in the surface air layer are pronounced? If significant differences exist, what is their dynamics?

## 1. MATERIALS AND METHODS

This study is based on data from three air monitoring stations: TOR stations ( $56^{\circ}28' N$ ,  $85^{\circ}03' E$ ), Fonovaya Observatory ( $56^{\circ}25' N$ ,  $84^{\circ}04' E$ ), and Basic Experimental Complex (BEC) ( $56^{\circ}28' N$ ,  $85^{\circ}06' E$ ) of V.E. Zuev Institute of Atmospheric Optics, Siberian Branch, Russian Academy of Sciences (Fig. 1). These posts are located under the same conditions. They are surrounded by mixed forest and are sufficiently distant from strong anthropogenic sources of air pollutants. The latter allows neglecting the impact of these sources on measurement data in most cases. One can see in Fig. 1 that the posts are lined up, which enables estimating the anthropogenic contribution of Tomsk to the formation of the field of atmospheric impurities in the presence of west-east transport of air masses.

To study the dynamics of surface air composition, the time series of hourly average concentrations of gases for 2013–2017 were analyzed. The choice of that time period was due to the fact that the posts full operated during that period. In 2018, due to a lightning strike, BEC failed and cannot be restored to its previous state for different reasons.

All three posts are equipped with automatic systems for measuring meteorological parameters and gas and aerosol concentrations in the surface air layer. Fonovaya Observatory and BEC are additionally equipped with Unzha-2 masts with corresponding sensors at several altitudes. Air is sampled at the TOR station at an altitude of 10 m above the ground and at Fonovaya Observatory and BEC at 10 and 30 m. Measurements are taken hourly and around the clock at all the stations.

The monitoring posts were created at different times and within different programs; therefore, they use different equipment. The list of devices is given in Table 1. Twelve different devices were used to record six atmospheric gases. At TOR station and BEC,  $O_3$  and  $NO/NO_2$  concentrations were measured by gas analyzers of the same type. Only one gas (CO) was measured with the same device at all the posts.

An important aspect of studying mesoscale differences in air composition is the measurement accuracy (uncertainty) of gases under study. The accuracy characteristics of the devices are given in Table 2.

In accordance with WMO requirements, to reduce the uncertainty of  $CO_2$  and  $SN_4$  measurements, daily calibrations were carried out using calibration gas mixtures of Deuste Steiner GmbH at Fonovaya Observatory and of the National Institute for Environmental Studies (NIES, Japan) at TOR station and BEC. The  $NO$ ,  $NO_2$ , and  $SO_2$  gas analyzers were calibrated daily using microflow capsules manufactured at D.I. Mendeleev All-Russian Scientific Research Institute of Metrology, by introducing the flow of impurities generated by them into purified air. The OPTEK 3.02-P and Model 49 ozone analyzers were calibrated using

**Table 1.** Devices used at the atmospheric composition monitoring posts

Gas	TOR station	BEC	Fonovaya Observatory
CO <sub>2</sub>	LGR FGGA Model 907-0010	LI-COR LI-820	Picarro G2301-m
CH <sub>4</sub>	LGR FGGA Model 907-0010	Figaro TGS-2611	Picarro G2301-m
O <sub>3</sub>	OPTEK 3.02-P	OPTEK 3.02-P	Thermo Model 49
NO/NO <sub>2</sub>	Teledyne API 200E	Teledyne API 200E	Model 42i-TL
CO	OPTEK K-100	OPTEK K-100	OPTEK K-100
SO <sub>2</sub>	Teledyne API 100E	ME 9850B	Model 43i-TLE

**Table 2.** Specification of the devices

Device	Gas	Concentration measurement range	Uncertainty
LGR FGGA Model 907-0010	CO <sub>2</sub> , ppm	20–10000	±0.2 ppm
LGR FGGA Model 907-0010	CH <sub>4</sub> , ppm	0.005–50	±0.001 ppm
Picarro G2301-m	CO <sub>2</sub> , ppm	0–1000	<0.2 ppm
Picarro G2301-m	CH <sub>4</sub> , ppm	0–20	<0.0015 ppm
LI-COR LI-820	CO <sub>2</sub> , ppm	0–1000	<0.2* ppm
Figaro TGS-2611	CH <sub>4</sub> , ppm	1–10	<0.007* ppm
OPTEK 3.02-P	O <sub>3</sub> , µg/m <sup>3</sup>	0–500	±20%
Thermo Model 49	O <sub>3</sub> , ppb	0–1000	±1 ppb
Teledyne API 200E	NO/NO <sub>2</sub> , ppm	0–20	±0.5%
Model 42i-TL	NO/NO <sub>2</sub> , µg/m <sup>3</sup>	0–10/500	±1%
OPTEK K-100	CO, mg/m <sup>3</sup>	0–50	±20%
Teledyne API 100E	SO <sub>2</sub> , ppm	0–20	±0.5%
ME 9850B	SO <sub>2</sub> , ppm	0–20	±1%
Model 43i-TLE	SO <sub>2</sub> , µg/m <sup>3</sup>	0–20/2000	±1%

\* When calibrating with test gas mixtures.

the GS-024 ozone generator (OPTEK JSC) once a month.

The WMO has specified unambiguous requirements for the measurement uncertainties for many hydrometeorological parameters already in the 20th century. These requirements were based on long-term studies of their spatiotemporal variability summarized in [23]; they are still in force and are presented in [24]. There are no such clear requirements for the uncertainties of measuring atmospheric gas components, with the exception of recommendations for monitoring greenhouse gases [25]. As follows from Table 2, most of the gas components under study were measured with uncertainties close to WMO recommendations. At two posts, the uncertainties of CO and O<sub>3</sub> concentrations significantly exceed the recommended values.

It is also important to consider the peculiarities of the study of the difference in the atmospheric parameters noted in [23]. The difference in two series with the periodic variability characteristic of the atmosphere has different signs in the corresponding time intervals under normal distribution of the parameter. The average difference in the concentrations of one gas tends to zero. Therefore, when analyzing meso-scale differences, the comparison should be made with the absolute values of their averages in the corresponding period. Let us explain this using Fig. 2 as an example.

Figure 2a shows the daily variation in SO<sub>2</sub> concentration over Fonovaya Observatory to be opposite to those over TOR station and BEC. The corresponding differences in the concentrations in Figs. 2a are 2b show completely different behavior. Thus, the TOR – BEC difference is negative during the day, and the

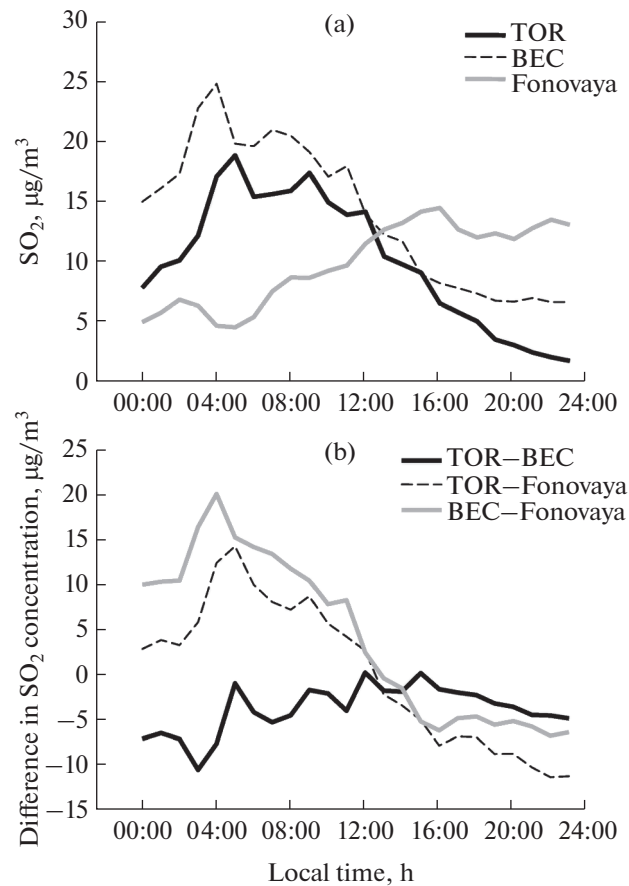


**Fig. 2.** (a)  $\text{SO}_2$  concentrations and (b) their differences at the TOR station, BEC, and Fonovaya Observatory on July 1, 2013.

TOR – Fonovaya and BEC – Fonovaya differences are positive in the first half and negative in the second half. This results in significantly different estimates of daily average differences and standard deviations (Table 3).

Table 3 shows that the average differences in concentrations between the stations calculated with consideration of the sign are underestimated by several (TOR – BEC and BEC – Fonovaya) and even tens (TOR – Fonovaya) of times. If the sign is ignored, then the standard deviations are reduced.

Gaps in long-term data series can be due to power outages, equipment failure, or equipment repair or calibration. If more than 20% of the data was missing in any period, this period was excluded from the processing.

## 2. RESULTS AND DISCUSSION

### 2.1. Long-Term Differences

Table 4 shows the average differences in concentrations between the three posts throughout the period under study (2013–2017) and the maximal and minimal differences between individual hourly readings over that time period. Plus (minus) means that the concentration is higher at the first (second) post.

It is evident that the long-term average differences in concentrations are significantly higher than the uncertainties of single measurements given in Table 2. Depending on the measurement site, they can differ by up to three times for certain components. This can reflect the effect of local factors: properties of the underlying surface and characteristics of vegetation on it, local air circulation, the presence of sources and

**Table 3.** Daily average values  $\pm$  SD of the difference in  $\text{SO}_2$  concentrations at the three stations with and without taking into account the sign

Calculation	TOR – BEC	TOR – Fonovaya	BEC – Fonovaya
Taking into account the sign	$-3.84 \pm 2.65$	$0.25 \pm 8.06$	$4.09 \pm 9.04$
Without taking into account the sign	$3.87 \pm 2.60$	$7.17 \pm 3.37$	$8.49 \pm 4.90$

**Table 4.** Long-term average (2013–2017) differences in gas concentrations at the TOR station, Fonovaya Observatory, and BEC

Gas	TOR – Fonovaya		BEC – Fonovaya		TOR – BEC	
	average $\pm$ SD	range	average $\pm$ SD	range	average $\pm$ SD	range
CO, $\mu\text{g}/\text{m}^3$	195 $\pm$ 146	–2658 +2457	116 $\pm$ 135	–1887 +1670	155 $\pm$ 134	–1819 +2394
CO <sub>2</sub> , ppm	8.3 $\pm$ 9.2	–137 +217	5.5 $\pm$ 7.5	–155 +165	3.3 $\pm$ 3.0	–164 +136
NO, $\mu\text{g}/\text{m}^3$	0.8 $\pm$ 0.9	–21 +23	0.7 $\pm$ 1.1	–20 +35	0.4 $\pm$ 1.0	–29 +21
NO <sub>2</sub> , $\mu\text{g}/\text{m}^3$	7.4 $\pm$ 6.5	–109 +96	4.6 $\pm$ 6.0	–117 +100	15.5 $\pm$ 7.6	–83 +90
O <sub>3</sub> , $\mu\text{g}/\text{m}^3$	13.4 $\pm$ 10.7	–116 +116	8.1 $\pm$ 7.0	–95 +88	14.3 $\pm$ 10.6	–94 +117
SO <sub>2</sub> , $\mu\text{g}/\text{m}^3$	6.9 $\pm$ 3.5	–97 +63	2.3 $\pm$ 2.4	–92 +32	5.7 $\pm$ 2.8	–40 +84

**Table 5.** Long-term average gradients of gas concentrations (C/km) at the TOR station, Fonovaya Observatory, and BEC

Gas	TOR – Fonovaya	BEC – Fonovaya	TOR – BEC
CO, $\mu\text{g}/\text{m}^3$	3.48	1.93	38.75
CO <sub>2</sub> , ppm	0.15	0.09	0.83
NO, $\mu\text{g}/\text{m}^3$	0.014	0.012	0.100
NO <sub>2</sub> , $\mu\text{g}/\text{m}^3$	0.13	0.08	3.88
O <sub>3</sub> , $\mu\text{g}/\text{m}^3$	0.24	0.14	3.58
SO <sub>2</sub> , $\mu\text{g}/\text{m}^3$	0.12	0.04	1.43

sinks of individual gases or their precursors, etc. This witnesses real mesoscale differences in the atmospheric composition in the region under study. Since hourly data over a five-year period were used for the assessment (>43000 values), the standard deviations are quite large and comparable with the averages. This is also characteristic of other atmospheric parameters [23, 24]. The maximal and minimal deviations of concentrations from the averages are almost symmetrical, which indicates the absence of a constant difference between the measurement sites. The differences in concentrations are higher than the average values by an order of magnitude or more. However, it should be taken into account that we did not exclude from the analysis the situations of frontal passages over the city, which abruptly and significantly increased the concentrations of impurities [26]; fires, etc.

The average differences in concentrations given in Table 4 do not contradict literature data. According to [27], the annual average difference between CO<sub>2</sub> concentrations at four background China stations attained 13 ppm in 2011. The difference in CO<sub>2</sub> concentrations

at five Finnish stations averaged 5–10 ppm in winter [28]. The annual average difference between CO<sub>2</sub> concentrations at six posts in Western Siberia was equal to 11 ppm in 2016 [29]. The winter (summer) differences in atmospheric gas concentrations at points spaced 50 km apart were 157 (47)  $\mu\text{g}/\text{m}^3$  for NO, 43 (31)  $\mu\text{g}/\text{m}^3$  for NO<sub>2</sub>, 11 (12)  $\mu\text{g}/\text{m}^3$  for SO<sub>2</sub> [30]. The differences in ozone concentrations can attain 50  $\mu\text{g}/\text{m}^3$  at points spaced 50 km apart, and the ratio of their monthly averages can vary by two to four times [31].

The differences in the concentrations given in Table 4, like in the cited works, have been calculated with neglect of the distances between TOR station and Fonovaya Observatory (56 km), BEC and Fonovaya (60 km), TOR and BEC (4 km), which complicates their comparison. Therefore, these data are reduced to a single distance in Table 5. Let us recall that the mesoscale is divided into three categories: meso- $\alpha$  (200–2000 km), meso- $\beta$  (20–200 km), and meso- $\gamma$  (2–20 km) [15]. Therefore, the first two differences

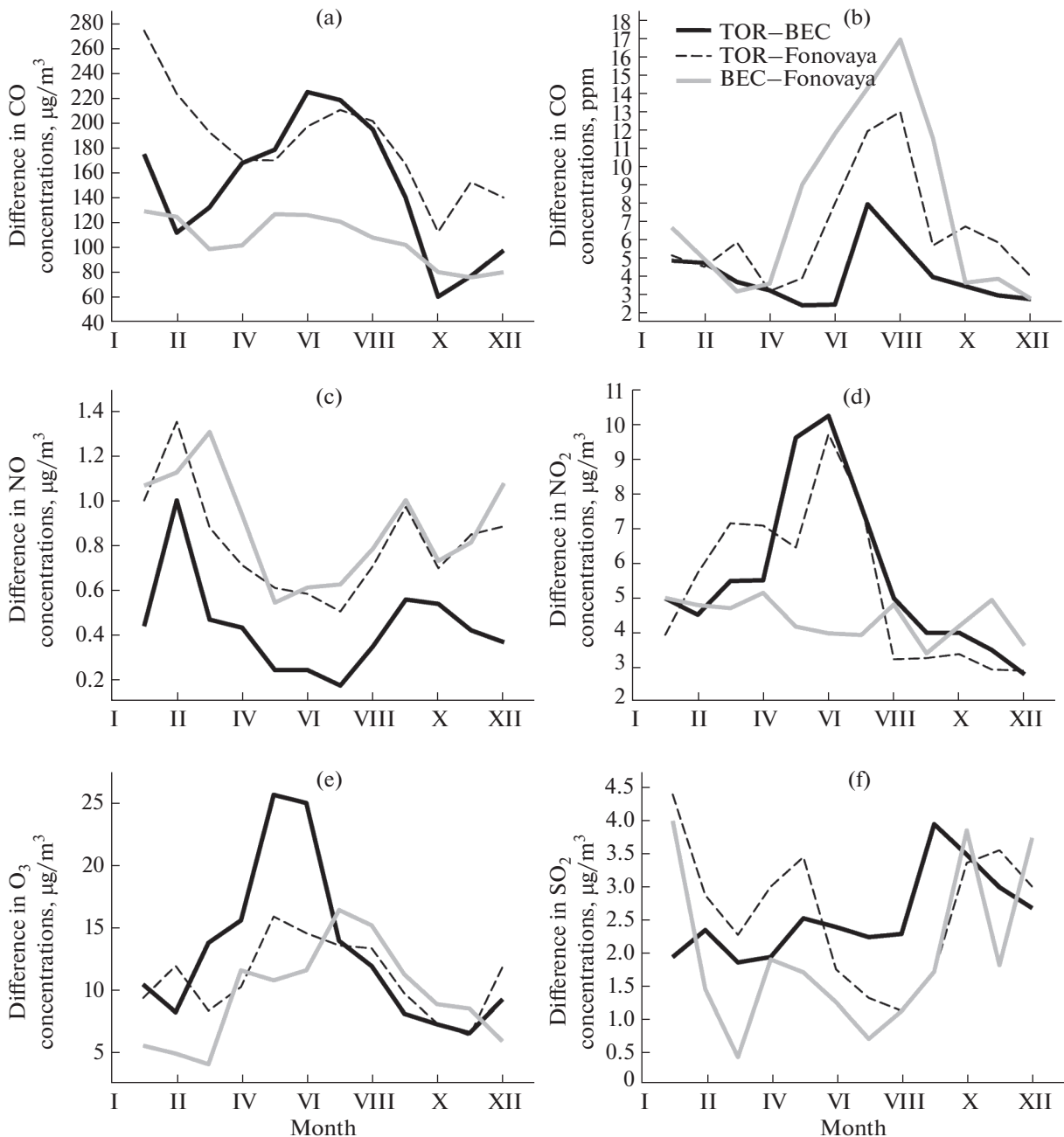


**Fig. 3.** Long-term average annual variations in the difference in the concentrations (a) CO, (b) CO<sub>2</sub>, (c) NO, (d) NO<sub>2</sub>, (e) O<sub>3</sub>, and (f) SO<sub>2</sub> at the TOR station, BEC, and Fonovaya Observatory.

(TOR – Fonovaya and TOR – BEC) relates to mesoscale  $\beta$ , and the difference TOR – BEC relates to mesoscale  $\gamma$ .

Table 5 shows that the gradients of the concentration differences are comparable on mesoscale  $\beta$  and sharply increase on mesoscale  $\gamma$ . It is difficult to say whether this obeys some law. We found only one publication devoted to this issue [32], where an ozone gradient of 8–23 ppb was obtained. But this result relates to special conditions, that is, a decrease in the concen-

tration with distance from the shore within the breeze system.

## 2.2. Annual Dynamics

Temporal variations in the differences in gas concentrations between observation posts near Tomsk are shown in Fig. 3. Figure 3a shows two maxima, winter and summer, and two minima, spring and autumn, in the annual dynamics of the differences in CO concen-

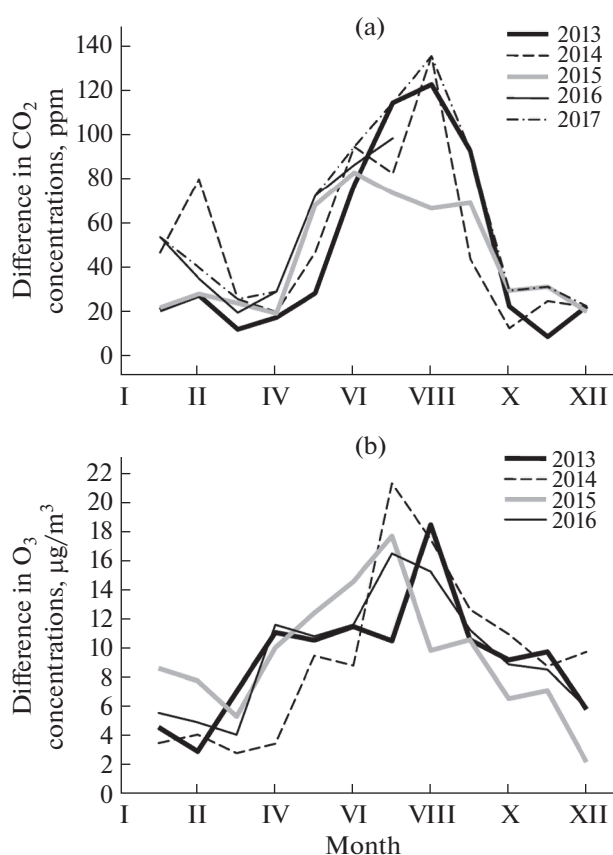


Fig. 4. Monthly average differences in the concentrations of (a) CO<sub>2</sub> and (b) O<sub>3</sub> at BEC and Fonovaya Observatory.

trations, which is significantly different from the annual dynamics of surface CO concentration. Works [33–35] show its maximum in spring and minimum in summer. It is difficult to explain this behavior of concentration differences on the mesoscale. It can only be noted that the differences in concentrations and the amplitude of deviations do not depend on the distance between sites. It is possible that TOR station is affected by anthropogenic sources, since it is located in a suburban area. We hope to answer this question in the next study.

The CO<sub>2</sub> concentrations vary the strongest in summer because of active absorption of CO<sub>2</sub> by vegetation during photosynthesis in daytime and its significant emission during respiration at night [29]. This is also manifested in the differences in its concentrations in Fig. 3b. The differences are evidently maximal in summer. Different amplitudes can be explained by different plants growing around the observation sites.

Before analyzing the differences in concentrations of the following gas components, let us recall that NO–O<sub>3</sub>–NO<sub>2</sub> photochemical equilibrium is usually established in the clear troposphere [36–38]:

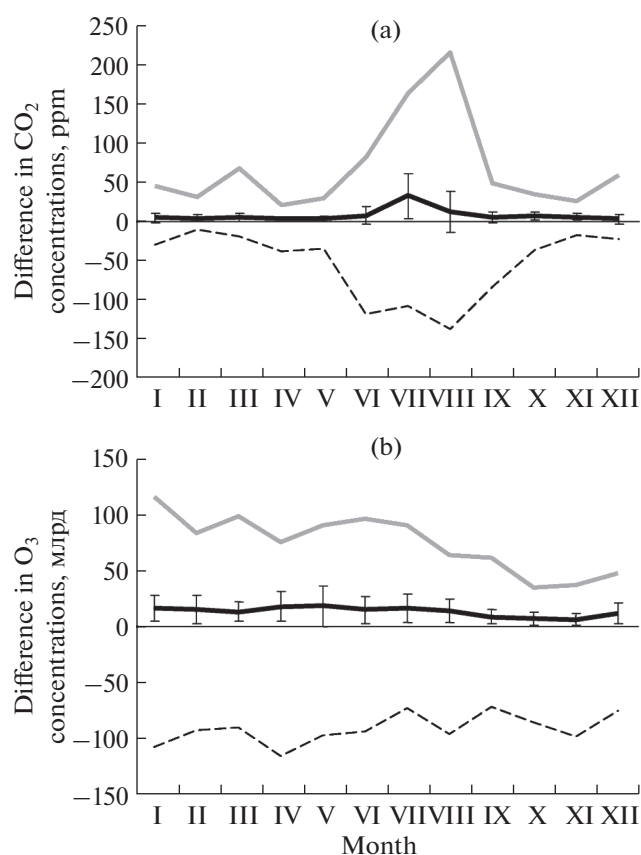
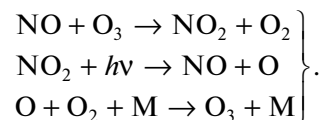
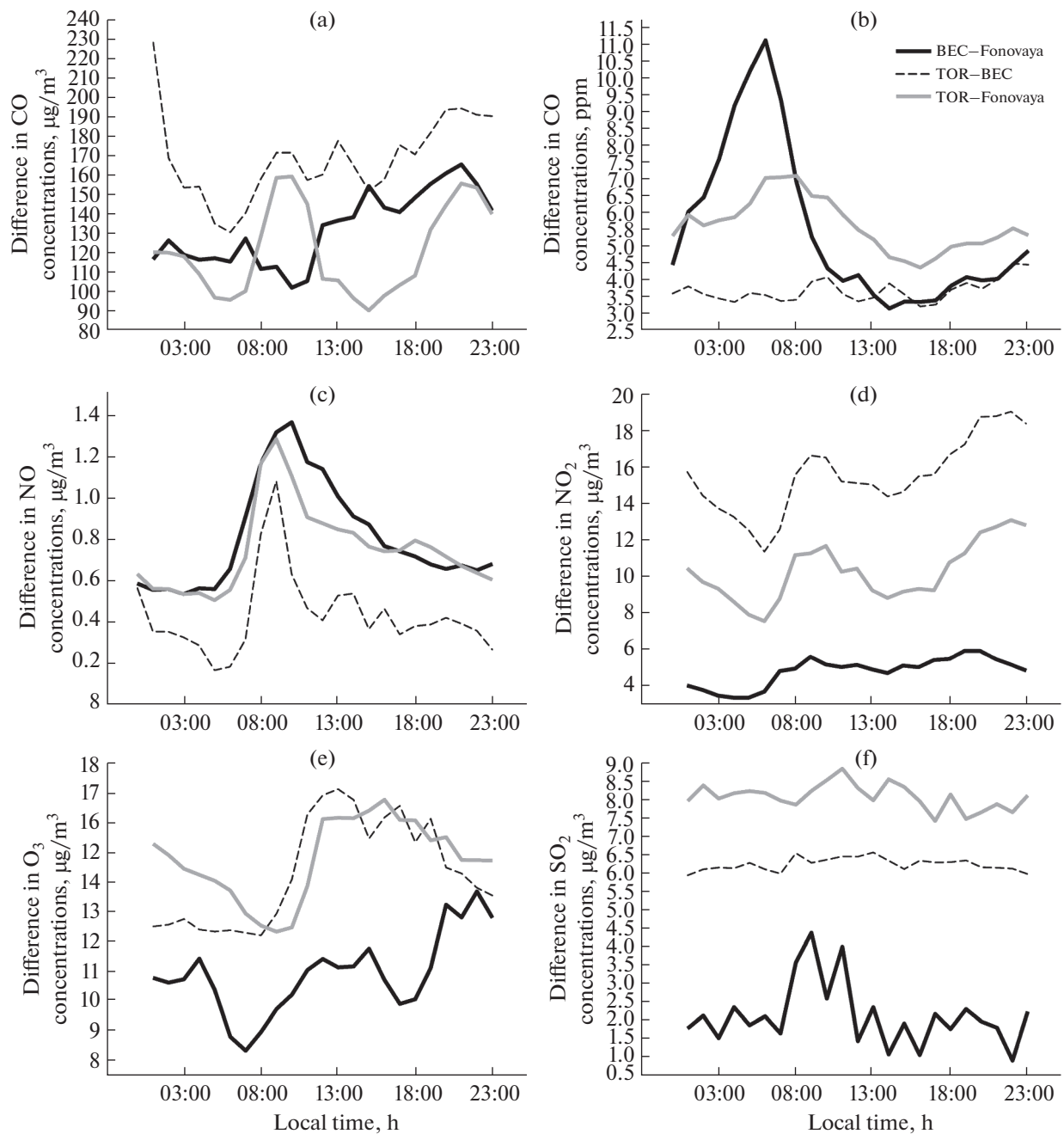


Fig. 5. Monthly average differences, standard deviations, and positive and negative deviations of (a) CO<sub>2</sub> and (b) O<sub>3</sub> at TOR station and Fonovaya Observatory.



Our previous study [39] found low NO concentrations in the region due to very weak N<sub>2</sub>O fluxes from the soil to the atmosphere [40]. Under these conditions, a small amount of released N<sub>2</sub>O is converted into NO in the atmosphere and is quickly converted into NO<sub>2</sub> during photochemical processes. As a result, very low NO concentrations are recorded in background regions, since most of NO is converted into NO<sub>2</sub>, and the amount of ozone is determined by the release of hydrocarbons mainly of natural origin. During a year, the concentration of NO has a maximum in the cold season, while NO<sub>2</sub> and O<sub>3</sub> concentrations peak in spring/summer, when photochemical processes are the most active.

All of the above said is confirmed by Figs. 3c–3e. Thus, the differences for NO (Fig. 3c) are small in the warm period and increase in the cold period. Maximal differences in NO<sub>2</sub> (Fig. 3d) and O<sub>3</sub> (Fig. 3e) concentrations are seen in spring or summer.



**Fig. 6.** Long-term average daily variation in the difference in the concentrations of (a) CO, (b) CO<sub>2</sub>, (c) NO, (d) NO<sub>2</sub>, (e) O<sub>3</sub>, and (f) SO<sub>2</sub> at TOR station, BEC, and Fonovaya Observatory.

Low concentrations of SO<sub>2</sub> in the region cause small differences between the stations (Fig. 3f). The differences for this gas, as well as for NO, are characterized by a decrease in the warm period and an increase in the cold period, although no annual trend is pronounced.

The temporal stability of the above trends can be traced for BEC – Fonovaya difference (Fig. 4) as an

example. Variations in differences both within and between years are seen, but the general trend holds.

It is also necessary to analyze the behavior of the differences in concentrations during a year (Fig. 5). The increase in the monthly average differences in CO<sub>2</sub> and ozone is evidently due to the increase in the range of their deviations from the averages. Since no such studies were previous performed for the atmo-

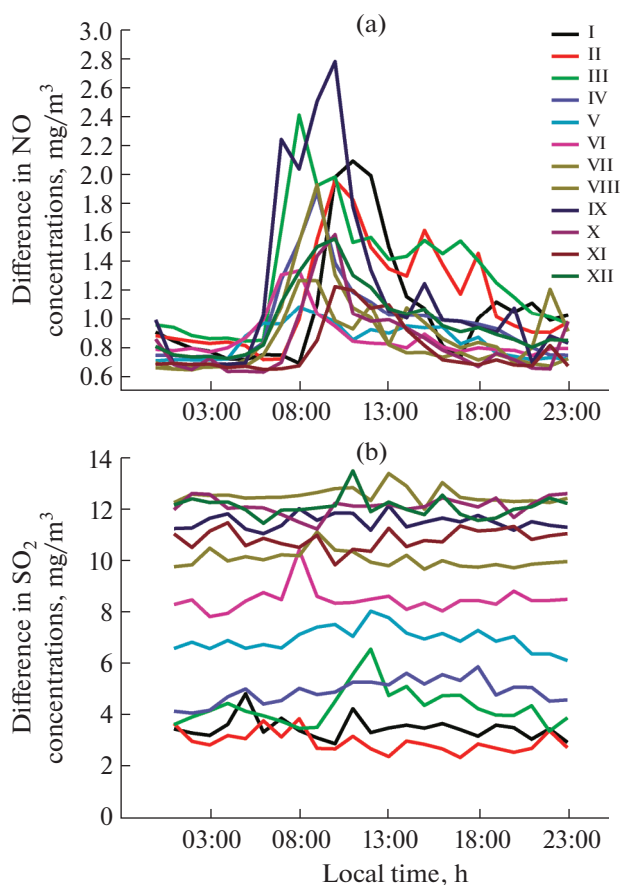


Fig. 7. Long-term daily average variations in the difference in the concentrations of (a) NO and (b) SO<sub>2</sub> at BEC and Fonovaya Observatory in different months.

spheric composition, it is not yet possible to compare our data with other results.

### 2.3. Daily Dynamics

The atmospheric processes which determine air composition change during the day. In the daytime, vegetation absorbs carbon dioxide during photogenesis. At night, when there is no light, vegetation switches to breathing and returns CO<sub>2</sub> back to the atmosphere. During the day, photochemical processes start and not only produce ozone, but also change the balance of nitrogen oxide concentrations. Heating of the surface during daytime and its cooling at night significantly affect the soil–atmosphere gas exchange. Hence, it is interesting to consider how they affect the differences in gas concentrations, which should reflect local features. Such data are shown in Fig. 6.

According to Fig. 6a, the differences in CO concentrations at the stations behave differently. Except for TOR – Fonovaya difference, they generally tend to increase during daytime and decrease at night. The significant difference between TOR station and BEC at night can be due to the effect of urban emissions.

The differences in CO<sub>2</sub> concentrations (Fig. 6b) increase at all the stations at night and decrease during the day. This is especially true for closely located TOR station and BEC. This behavior can only be explained by the difference in plants surrounding the observation sites, some of which release a larger amount of CO<sub>2</sub> in respiration.

The differences in NO concentrations at all the three stations similarly behave during the day (Fig. 6c). The morning maximum in N<sub>2</sub>O concentration is caused by the conversion of NO to NO<sub>2</sub> in the morning hours due to the start of photochemical ozone generation [41]. This behavior of NO concentration differences is due to the low rate of supply of its precursor N<sub>2</sub>O in the region [40].

Different daily variations in NO<sub>2</sub> concentration differences (Fig. 6d) reflect, on the one hand, the above-mentioned morning conversion of NO to NO<sub>2</sub>, which manifests itself as a maximum. The second maximum in the evening is caused by the sink of ozone from the atmosphere [41]. The stable difference between the stations during the day is most likely due to the different power of the sources of ozone precursors, in the generation of which nitrogen oxides function as “switches” of chains [42, 43].

The daily variations in the differences in ozone concentrations in Fig. 6e show its day and night maxima at each point [41]. The differences in their values are obviously due to the amount of organic precursors emitted by different plants at each point.

The differences in SO<sub>2</sub> concentrations (Fig. 6f) at all the points show neutral daily behavior. Actually, the TOR – BEC difference has a small morning maximum, the nature of which is to be ascertained. The difference between the three curves is stable during the day, which might well be due to the different nature of SO<sub>2</sub> exchange between the soil and the atmosphere.

At most stations, the above differences hold throughout the year. Let us show this in Fig. 7. The daily variations in the difference in NO concentrations throughout a year in Fig. 7a are similar to the long-term daily average variations in Fig. 6c. The differences in SO<sub>2</sub> concentrations behave in a similar way (Fig. 7b). Their daily variations coincide in nature with those in Fig. 6f. In Fig. 7, variations in the concentration differences, previously noted in section 2.2, are clearly visible.

The daily variations in the differences in concentrations are similar in different years (Fig. 8), but the amplitudes of the variations differ.

## CONCLUSIONS

The study has shown that there are real mesoscale differences in the atmospheric composition in the region under study, which reflects the action of local factors: properties of the underlying surface and vege-

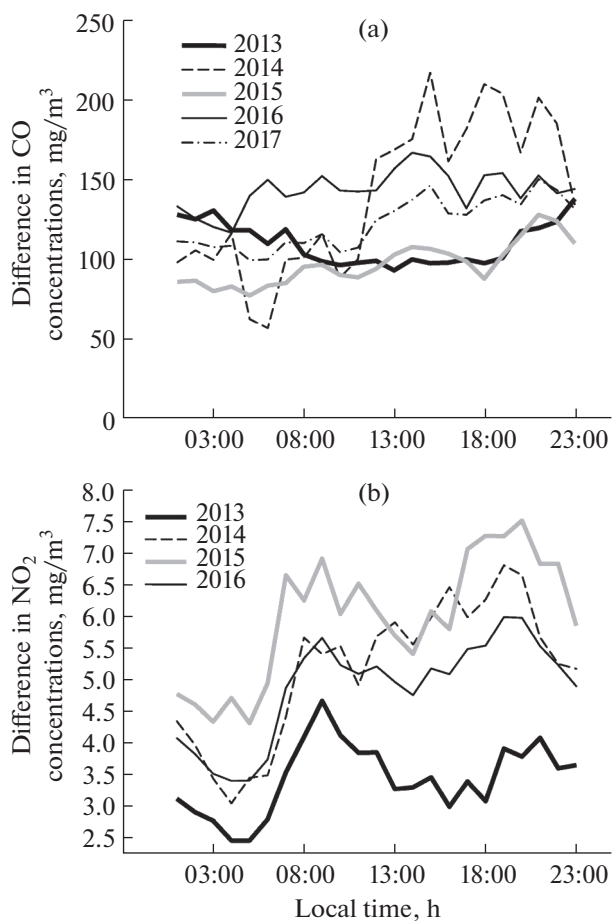


**Fig. 8.** Daily average variations in the differences in the concentrations of (a) CO and (b) NO<sub>2</sub> at BEC and Fonovaya Observatory in different years.

tation, local air circulation, the presence of sources and sinks of individual gases or their precursors, etc.

Long-term average differences in concentrations are significantly higher than the uncertainties of single measurements. Depending on the measurement site, they can differ by up to three times for some gas components. An assessment of the gradients of concentration differences shows that they are comparable on mesoscale  $\beta$  and sharply increase on mesoscale  $\gamma$ .

In the annual dynamics, the differences in CO<sub>2</sub>, NO<sub>2</sub>, and O<sub>3</sub> concentrations show maxima in the warm season, and in NO and SO<sub>2</sub> concentrations, in the cold season. The dynamics of CO concentration reflects local features of gas sources and sinks. The identified regularities are stable over many years.

The daily dynamics of the differences in CO concentrations is characterized by a general trend at all the stations, that is, an increase during daytime and a decrease during dark hours. For SO<sub>2</sub>, an increase in the differences in the concentrations at night and a decrease during the day are typical at all stations, which can only be explained by different plants grow-

ing around, some of which release more CO<sub>2</sub> in respiration. The differences in NO concentrations similarly behave during the day at all the three stations, i.e., the presence of a morning maximum due to NO conversion into NO<sub>2</sub> in the morning hours after the start of photochemical ozone generation. This behavior is due to the low rate of supply of its precursor N<sub>2</sub>O in the region. Differences in the concentrations of O<sub>3</sub> are obviously caused by the amount of its organic precursors emitted by different plants at each site. The differences in SO<sub>2</sub> concentrations show neutral daily variations at all the points. The above differences hold throughout a year at most stations. The daily variations in the differences in concentrations are similar in different years.

#### FUNDING

The work was supported by the Ministry of Science and Higher Education of the Russian Federation (V.E. Zuev Institute of Atmospheric Optics, Siberian Branch, Russian Academy of Sciences).

#### CONFLICT OF INTEREST

The authors of this work declare that they have no conflicts of interest.

#### REFERENCES

1. "Summary for policymakers," in *Climate Change 2023: Synthesis Report. Contribution of Working Groups I, II, and III to the Sixth Assessment Report of the Intergovernmental Panel on Climate Change* (IPCC, Geneva, 2023), pp. 1–34. <https://doi.org/10.59327/IPCC/AR6-9789291691647>
2. M. Ramonet, Ph. Ciais, M. K. Sha, M. Steinbacher, C. Sweeney, "CO<sub>2</sub> in the atmosphere: Growth and trends since 1850," in *Oxford Research Encyclopedias of Climate Science* (Oxford, 2023), pp. 1–44. <https://doi.org/10.1093/acrefore/9780190228620.013.863>
3. A. A. Kiselev and I. L. Karol', *Life with Methane* (A.I. Voeikov Main Geophysical Observatory, St. Petersburg, 2019) [in Russian].
4. R. L. Thompson, L. Lassaletta, P. K. Patra, C. Wilson, K. C. Wells, A. Gressent, E. N. Koffi, M. P. Chipperfield, W. Winiwarter, E. A. Davidson, H. Tian, and J. G. Canadell, "Acceleration of global N<sub>2</sub>O emissions seen from two decades of atmospheric inversion," *Nat. Clim. Change* **9** (12), 993–998 (2019). <https://doi.org/10.1038/s41558-019-0613-7>
5. A. R. Desai, S. Paleri, J. Mineau, H. Kadum, L. Wanner, M. Mauder, B. J. Butterworth, D. J. Durden, and S. Metzger, "Scaling land–atmosphere interactions: Special or fundamental?," *J. Geophys. Res. Biogeosci.* **127** (9) (2022). <https://doi.org/10.1029/2022JG007097>
6. B. Deak, Z. Botta-Dukat, Z. Radai, B. Kovacs, I. Apostolova, Z. Batori, A. Kelemen, K. Lukacs, R. Kiss, S. Palpurina, D. Sopotlieva, and O. Valko,

- “Meso-scale environmental heterogeneity drives plant trait distributions in fragmented dry grasslands,” *Sci. Total Environ.* **947**, 174355 (2024).  
<https://doi.org/10.1016/j.scitotenv.2024.174355>
7. J. J. Lembrechts and I. Nijs, “Microclimate shifts in a dynamic world,” *Science* **368** (6492), 711–712 (2020).
  8. F. Zellweger, P. De Frenne, J. Lenoir, P. Vangansbeke, K. Verheyen, M. Bernhardt-Romermann, L. Baeten, R. Hedl, I. Berki, J. Brunet, H. Van Calster, M. Chudomelova, G. Decocq, T. Dirnbock, T. Durak, T. Heinken, B. Jaroszewicz, M. Kopecky, F. Malis, M. Macek, M. Malicki, T. Naaf, T. A. Nagel, A. Ortman-Ajkai, P. Petrik, R. Pielech, K. Reczynska, W. Schmidt, T. Standovar, K. Swierkosz, B. Teleki, O. Vild, M. Wulf, and D. Coomes, “Forest microclimate dynamics drive plant responses to warming,” *Science* **368** (6492), 772–775 (2020).  
<https://doi.org/10.1126/science.aba6880>
  9. A. M. Alferov, V. G. Blinov, M. L. Gitarskii, V. A. Grabar, D. G. Zamolodchikov, A. V. Zinchenko, N. P. Ivanova, V. M. Ivakhov, R. T. Karabanyu, D. V. Karelin, I. L. Kalyuzhnyi, F. V. Kashin, D. E. Konyushkov, V. N. Korotkov, V. A. Krovotyntsev, S. A. Lavrov, A. S. Marunich, N. N. Paramonova, A. A. Romanovskaya, A. A. Trunov, A. V. Shilkin, and A. K. Yuzbekov, *Monitoring of Greenhouse Gas Fluxes in Natural Ecosystems* (Amirit, Saratov, 2017) [in Russian].
  10. D. Shi, Y. Jiang, W. Li, Y. Wen, F. Wu, and S. Zhao, “Spatial-temporal heterogeneity of spring phenology in boreal forests as estimated by satellite solar-induced chlorophyll fluorescence and vegetation index,” *Agric. Forest Meteorol.* **346**, 109888 (2024).  
<https://doi.org/10.3390/ijerph182413031>
  11. A. V. Olchev, Yu. V. Mukhartova, N. T. Levashova, M. S. Ryzhova, P. A. Mangura, and E. M. Volkova, “The influence of the spatial heterogeneity of vegetation cover and surface topography on vertical CO<sub>2</sub> fluxes within the atmospheric surface layer,” *Izv., Atmos. Ocean. Phys.* **53** (5), 539–549 (2017).
  12. Y. Cao, X. Yue, H. Liao, X. Wang, Y. Lei, and H. Zhou, “Impacts of land cover changes on summer surface ozone in China during 2000–2019,” *Sci. Total Environ.* **948**, 174821 (2024).  
<https://doi.org/10.1016/j.scitotenv.2024.174821>
  13. A. V. Smagin and D. V. Karelin, “Effect of wind on soil–atmosphere gas exchange,” *Eurasian Soil Sci.* **54** (3), 372–380 (2021).
  14. O. C. Acevedo, Moraes O. L. L. Osvaldo, G. A. Degrazia, D. R. Fitzjarrald, A. O. Manzi, and J. G. Campos, “Is friction velocity the most appropriate scale for correcting nocturnal carbon dioxide fluxes?,” *Agric. Forest Meteorol.* **149** (1), 1–10 (2009).  
<https://doi.org/10.1016/j.agrformet.2008.06.014>
  15. S. N. Stepanenko, *Mesometeorology* (OGMI, Odessa, 2001) [in Russian].
  16. *Review of the State and Pollution of the Environment in the Russian Federation in 2019* (Roshydromet, 2020) [in Russian].
  17. J. P. Burrows and R. Martin, “Satellite observations of tropospheric trace gases and aerosols. Introduction,” *IGAC Newsletter*, No. **35**, 2–7 (2007).  
[https://doi.org/10.1007/978-94-011-4353-0\\_27](https://doi.org/10.1007/978-94-011-4353-0_27)
  18. J. Tollefson, “Carbon-sensing satellite system faces high hurdles,” *Nature* **533** (7604), 446–447 (2016).  
<https://doi.org/10.1038/533446a>
  19. G. Popkin, “Commercial space sensors go high-tech,” *Nature* **545** (7655), 397–398 (2017).
  20. R. R. Gibadullin, Yu. V. Mukhartova, M. V. Kochkina, E. M. Satosina, V. M. Stepanenko, I. A. Kerimov, S. K. Gulev, and A. V. Olchev, “Modeling the spatial variability of the wind field and CO<sub>2</sub> and CH<sub>4</sub> fluxes over a heterogeneous surface,” *Russ. Meteorol. Hydrol.* **49** (9), 828–844 (2024).  
<https://doi.org/10.3103/S1068373924090085>
  21. A. Berchet, I. Pison, F. Chevallier, J.-D. Paris, P. Bousquet, J.-L. Bonne, M. Yu. Arshinov, B. D. Belan, C. Cressot, D. K. Davydov, E. J. Dlugokencky, A. V. Fofonov, A. Galanin, J. Lavric, T. Machida, R. Parker, M. Sasakawa, R. Spahni, B. D. Stocker, and J. Winderlich, “Natural and anthropogenic methane fluxes in Eurasia: A meso-scale quantification by generalized atmospheric inversion,” *Biogeosci.* **12** (18), 5393–5414 (2015).  
<https://doi.org/10.5194/bg-12-5393-2015>
  22. O. Yu. Antokhina, P. N. Antokhin, V. G. Arshinova, M. Yu. Arshinov, B. D. Belan, S. B. Belan, D. K. Davydov, N. V. Dudorova, G. A. Ivlev, A. V. Kozlov, T. M. Rasskazchikova, D. E. Savkin, D. V. Simonenkov, T. K. Sklyadneva, G. N. Tolmachev, and A. V. Fofonov, “Study of air composition in different air masses,” *Atmos. Ocean. Opt.* **32** (1), 72–79 (2019).
  23. V. D. Reshetov, *Variability of Meteorological Elements in the Atmosphere* (Gidrometeoizdat, Leningrad, 1973) [in Russian].
  24. *On the Composition, Accuracy, and Spatiotemporal Resolution of Information Necessary for Hydrometeorological Support of the National Economy and the Hydrometeorological Forecasting Service*, Ed. by M.A. Petrosyants and V.D. Reshetov (Gidrometeoizdat, Leningrad, 1975) [in Russian].
  25. *The 19th WMO/IAEA Meeting of Experts on Carbon Dioxide, Other Greenhouse Gases and Related Tracers Measurement Techniques. GAW Report no. 242* (WMO, 2018).
  26. K. L. Antonov, E. A. Gulyaev, Yu. I. Markelov, and V. A. Poddubny, “Variation patterns of CO<sub>2</sub> and CH<sub>4</sub> according to the measurements in the surface atmosphere over urban and suburban areas in 2021–2022,” *Russ. Meteorol. Hydrol.* **49** (5), 456–466 (2024).  
<https://doi.org/10.3103/S1068373924050091>
  27. S. X. Fang, L. X. Zhou, P. P. Tans, P. Ciais, M. Steinbacher, L. Xu, and T. Luan, “In situ measurement of atmospheric CO<sub>2</sub> at the four WMO/GAW stations in China,” *Atmos. Chem. Phys.* **14** (5), 2541–2554 (2014).  
<https://doi.org/10.5194/acpd-13-27287-2013>
  28. J. Kilkki, T. Aalto, J. Hatakka, H. Portin, and T. Laurila, “Atmospheric CO<sub>2</sub> observations at Finnish urban and rural sites,” *Boreal Environ. Res.* **20** (2), 227–242 (2015).
  29. D. Belikov, M. Arshinov, B. Belan, D. Davydov, and A. Fofonov, “Analysis of the diurnal, weekly, and seasonal cycles and annual trends in atmospheric CO<sub>2</sub> and CH<sub>4</sub> at tower network in Siberia during 2005–2016,”

- Atmosphere **10** (11), 698 (2019).  
<https://doi.org/10.3390/atmos10110689>
30. V. A. Obolkin, Yu. V. Shamanskii, T. V. Khodzher, and A. V. Falits, “Mesoscale processes of atmospheric pollutants transfer in the South Baikal region,” *Okeanologicheskie Issledovaniya* **47** (3), 104–113 (2019).
  31. W. R. Stockwell, R. M. Fitzgerald, D. Lu, and R. Perea, “Differences in the variability of measured and simulated tropospheric ozone mixing ratios over the Paso Del Norte region,” *J. Atmos. Chem.* **70** (1), 91–104 (2013).
  32. Y. Y. Huang and D. J. Donaldson, “Measurement report: Observations of ground-level ozone concentration gradients perpendicular to the Lake Ontario shoreline,” *Atmos. Chem. Phys.* **24** (4), 2387–2398 (2024).
  33. L. N. Yurganov, D. A. Jaffe, E. Pullman, and P. C. Novelli, “Total column and surface densities of atmospheric carbon monoxide in Alaska, 1995,” *J. Geophys. Res.* **103** (D15), 19337–19345 (1998).
  34. B. Barret, M. De Maziere, and E. Mahieu, “Ground-based FTIR measurements of CO from the Jungfraujoch: Characterization and comparison with in situ surface and MOPITT data,” *Atmos. Chem. Phys. Discuss.* **3** (5), 4857–4878 (2003).  
<https://doi.org/10.5194/acp-3-2217-2003>
  35. O. A. Tarasova, C. A. M. Brenninkmeijer, S. S. Assonov, N. F. Elansky, T. Rockmann, and M. A. Sofiev, “Atmospheric CO along the Trans-Siberian Railroad and River Ob: Source identification using isotope analysis,” *J. Atmos. Chem.* **57** (2), 135–152 (2007).
  36. W. L. Chameidas, D. D. Davis, J. Bradshaw, J. Sandholm, M. Rodgers, B. Baum, B. Ridley, S. Madronich, M. A. Carrol, G. Gregory, H. I. Schiff, D. R. Hastle, A. Torres, and E. Condon, “Observed and model-calculated NO<sub>2</sub>/NO ratios in tropospheric air sampled during the NASA GTE/CITE-2 field study,” *J. Geophys. Res.* **95** (D7), 10235–10247 (1990).
  37. J. V.-G. De Arellano and P. G. Duynkerke, “Influence of chemistry on the flux-gradient relationships for the NO–O<sub>3</sub>–NO<sub>2</sub> system,” *Bound.-Lay. Meteorol.* **61** (4), 375–387 (1992).
  38. J. H. Duyzer, G. Deinum, and J. Baak, “The interpretation of measurements of surface exchange of nitrogen oxides: Correction for chemical reactions,” *Phil. Trans. R. Soc. Lond. A* **351** (1696), 231–248 (1995).
  39. B. D. Belan, V. K. Kovalevskii, A. P. Plotnikov, and T. K. Sklyadneva, “Time behavior of the ozone and nitrogen oxides in the surface atmospheric layer near Tomsk,” *Atmos. Ocean. Opt.* **11** (12), 1139–1141 (1998).
  40. M. Yu. Arshinov, B. D. Belan, D. K. Davydov, A. V. Kozlov, and A. V. Fofonov, “Emission and sink of greenhouse gases in the grassland ecosystem of southern taiga of Western Siberia: Estimates of the contribution of soil flux component from observations of 2023,” *Atmos. Ocean. Opt.* **37** (6), 865–880 (2024).
  41. B. D. Belan, *Tropospheric Ozone* (Publishing House of IAO SB RAS, Tomsk, 2010) [in Russian].
  42. N. N. Semenov, *Chain Reactions* (Nauka, Moscow, 1986) [in Russian].
  43. G. I. Marchuk, *Numerical Simulation in Environmental Protection Problems* (OVM AN SSSR, Moscow, 1989) [in Russian].

**Publisher’s Note.** Pleiades Publishing remains neutral with regard to jurisdictional claims in published maps and institutional affiliations. AI tools may have been used in the translation or editing of this article.

SPELL: OK